International Journal of Engineering Sciences Paradigms and Researches (IJESPR)
Vol. 48, Special Issue, (TAME-2019, April 4-5, 2019)
(An Indexed, Referred and Impact Factor Journal approved by UGC- Journal No. 42581)
ISSN (Online): 2319-6564
www.ijesonline.com

INFLUENCE OF TOOL ROTATIONAL SPEED IN DISSIMILAR FRICTION STIR WELDING OF ALUMINIUM ALLOYS AA8011 AND AA5754 IN T-JOINT CONFIGURATION

Mubeen Ali1, Nabeel Ali1,*, Hashmatullah Ibrahimi1, Soumyashri Basu2, Zoya Imran1, Prakash Mishra1

**1Department of Mechanical Engineering, Jamia MilliaIslamia,
New Delhi-110025**

**2Department of Mechanical Engineering, Netaji SubhashUniversity of Technology,
New Delhi-110078
*Corresponding author email: nabeelali22@gmail.com**

Abstract

Friction stir welding has been successfully applied to join materials possessing application in various industrial sectors. Particularly, the T-joint configuration finds application in the aerospace and automotive sector. Thus, the aim of the present work is to study the effect of tool rotational speed on dissimilar Friction Stir Welding (FSW) of T-joint configuration. Aluminium alloys AA8011 and AA5754 having 3 mm thickness were used as base materials. Post welding, microstructural analysis and its correlation with micro-hardness was performed to study the effect of tool rotational speed, keeping the other welding parameters constant. Microstructural analysis was performed for both the skin and the stringer plates. Three distinct zones were realized, namely Stir zone (SZ), Thermo-mechanically affected zone (TMAZ) and Heat affected zone (HAZ). Tensile tests were also performed to examine the load-bearing capacity of the welded joint. The effect of rotational speed on weld defects has also been addressed in the current study.

Keywords**:** *Aluminium alloys; T-joint; Dissimilar Welding; Friction Stir Welding; AA8011; AA5754.*

1. Introduction

Friction Stir Welding (FSW) was developed and patented by TWI (1991) for the welding of high strength aluminium alloys [1]. Conventional fusion welding processes melt the base materials which in turn leads to solidification process resulting in distortion, residual stresses, severe metallurgical defects like porosity, inclusions, which reduces the joint efficiency of the base materials being welded. Thus, FSW a clean solid-state joining process is used to weld such hard to weld materials and eliminate the defects which arise due to conventional fusion welding processes. [2-3].

During FSW, the heat required to soften the base materials is generated due to the friction between the tool shoulder and the material as well as the plastic deformation of the base materials due to tool shoulder and tool pin. During FSW, the softened base material moves from the advancing side (AS) to the retreating side (RS) and finally consolidates at the back of the pin.

The FSWed joints comprise of three distinct zones, namely the nugget identified by the formation of equiaxed grains due to the continuous dynamic recrystallization, the Thermo-Mechanical Affected Zone (TMAZ) identified by severe deformation of the grains and the Heat Affected Zone (HAZ) [4-8]. Joints produced using FSW imparts excellent weld properties [9-11], which justifies its edge over the conventional fusion welding processes and promotes its use in the high technology industries i.e. railways, ship-building, automotive industry and aerospace industry. Welding of dissimilar materials is of importance to these industries because it enables to have the properties of both the base materials in a single component.

The significance of T-joint configuration typically lies with the aerospace and shipbuilding industries [12] for manufacturing panels and structural bodies of aircraft and ships, steel bridges and pressure vessels [13-14]. The T-joint is characterized by the welding of the horizontal plate (skin) to the vertical plate (stringer), hence strengthening the skin and providing the required strength to the structure without increasing its weight. 5xxx series of aluminium alloy contains Magnesium as the main alloying element hence, making it light in weight and imparts excellent corrosion resistance properties, thus making it ideal for use in the hull structures. The 8xxx series with alloying elements

as Iron and Silicon exhibit high strength to weight properties. The combination of the two aluminium alloys is a promising alternative for marine applications.

Dissimilar welding of aluminium alloys AA2024-T4 and AA6082-T6 in T-configuration was done by Fratini et al. [15] followed by the metallurgical and mechanical evaluation of the joints and calculation and comparison of the thermal and plastic flow fields. Zhao et al. [16] co-related the formation of tunnel defect with traverse speed and investigated the effect of tunnel defect and welding parameters on tensile properties of similar FSW of AA6013-T4. Cui et al. [17] carried out studies on the formation of kissing bond defect, tunnel defect, zigzag line defects in T-joints using macro-micro observations followed by their effect on the tensile strength of the weld. The fracture locations and surfaces were analyzed too for similar FSW of AA6061-T4.

T-joint welding has been an area of interest due to its importance for the various industries. A number of researchers have investigated the T-joint welding of aluminium alloys, whereas literature is scarce for dissimilar welding of aluminium alloys in T-joint configuration. Also, the pair used in the present study has not been addressed by any other researcher. In the present study, dissimilar aluminum alloys AA8011 and AA5754 have been welded in T-joint configuration using FSW. The objective of this study is to establish the effect of rotational speed to eliminate the defects in FSW of the specified pair and perform microstructure and microhardness analysis and tensile tests to establish a correlation of the mechanical properties with the microstructure of the welds.

2. Experimental Procedure

Aluminium alloys AA8011 and AA5754 plates having dimensions 180 mm*50 mm and thickness of 3 mm each were joined using FSW in T-joint configuration. The chemical composition of AA8011 and AA5754 are presented in Tables 1 and 2 respectively. The mechanical properties of the base materials are shown in Table 3. The AA8011 plate was placed as the skin (horizontal) and the AA5754 plate was placed as the stringer (vertically). High chromium high carbon (H13) was used as the tool material to perform the welds. The tool pin had a continuous tapered cylindrical profile. The tool geometry is shown in Figure 1. A robust vertical milling machine (make: BFW, Bangalore) retrofitted for performing FSW was used for the welding as shown in Figure 2.

Figure 1: FSW Tool

Figure 2: FSW Machine

During the welding, only the rotational speed was varied by keeping other parameters constant. The tool geometry was kept constant with a shoulder diameter of 18 mm, pin length of 2.8 mm tool tilt angle of 2.5°. The welding speed of 63 mm/ min was used along with the rotational speeds of 560 rpm and 900 rpm. The experimental plan is shown in Table 4.

Table 1: *Chemical Composition AA8011 (wt. %)*

Element	Fe	Cu	Mn	Zn	Ti	Cr	Al
AA8011	0.60-0.95	0.1-0.20	0.1-0.10	0.1-0.20	0.20-0.30	0.20-0.30	98

Table 2: *Chemical Composition AA5754 (wt. %)*

Element	Si	Cu	Mn	Cr	Zn	Mg	Mn+Cr	Fe	Al
AA5754	0.0-0.4	0.1	0.0-0.5	0.3	0.2	2.6-3.6	0.1-0.6	0.4	Balance

Table 3: *Mechanical Properties of base materials*

B M	AA5754	AA8011
Tensile strength(MPa)	227.8	137.8
Hardness (HV)	68.4	46

Table 4: *Experimental Plan*

Experiment Number	Rotational speed(rpm)	Welding speed (mm/min	Shoulder diameter(mm)

		)	
E1	560	63	18
E2	900	63	18

The samples for their characterization were procured using Wire Electron Discharge Machine (Wire-EDM). Samples for microstructural examination were prepared using standard metallographic techniques and etched with a suitable etchant. Microstructural analysis was done with the help of Optical Microscopy. Microhardness was measured for both the samples and for both skin and stringer plates with a load of 100 g applied for 15 s. Vickers microhardness was evaluated using Vickers micro-hardness tester (make: Mitutoyo, Japan) and tensile tests were performing using tensometer for the skin plates.

3. Results and Discussion

3.1 Macrostructure

The macrostructures of the welded samples are shown in Figure 3a and 3b for E1 and E2 respectively. It is clearly evident from the macrographs that a tunneling defect is observed in E1. As higher rotational speed induces more heat to the base materials during the welding process, hence E2 experiences a large thermal cycle in comparison to E1. The higher heat experienced by E2 might have led to better softening of the base materials and in turn resulting in lower flow stress and high flowability. Relatively lower flow stress contributes to better materials movement and in turn completion of the welded joint.

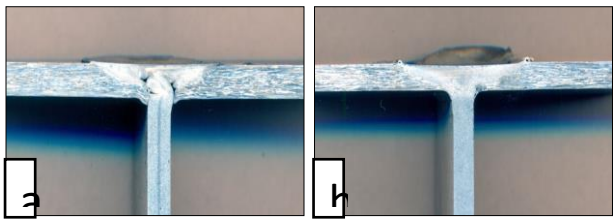

Figure 3: Macrographs a) E1 b) E2

3.2 Microstructure

For both E1 and E2, three zones are identified on the skin plates namely stir zone (SZ), thermos-mechanically affected zone (TMAZ) and heat affected zone (HAZ). The SZs of both welded samples (refer Figure 4) clearly depicts the presence of fine equiaxed dynamically recrystallized grains. The grains in SZ experiences both large thermal cycle as well as severe plastic deformation due to the rotating tool [18]. Adjacent to SZ is TMAZ, which is found on both advancing side (AS) and retreating side (RS) of the horizontal plate. The interface for SZ and TMAZ is more prominent on the AS. This is due to higher material deformation rate on the AS [19]. TMAZ experiences thermal cycle juxtaposing to SZ. This region consists of highly deformed grains as well as partially recrystallized grains. Hence, the grain size in TMAZ is relatively coarser in comparison to SZ as shown in Figure 5. Further moving towards the base material from TMAZ, HAZ is observed for both AS and RS (refer Figure 6). HAZ is a region experiencing only thermal cycle and does not undergo plastic deformation [20]. Welded samples realize minimum strength mainly due to coarsening of grains as well as dissolution and coarsening of strengthening precipitates.

The grains in E2 are found to be coarser (see Figure 4, 5 and 6), because E2 experiences a larger thermal cycle than E1. Higher rotational speed induces more heat and in turn, leading to coarsening of grains. Similar results have been observed by Khan et al. [21] while joining dissimilar aluminium alloys.

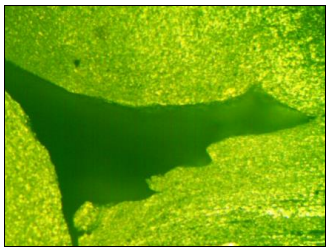

Figure 7: Tunnel Defect in E1

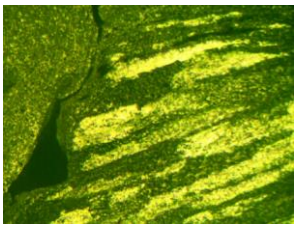

Figure 8: Hooking Defect in E2

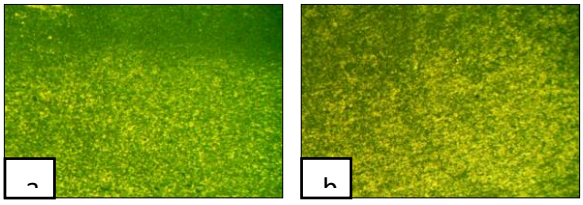

Figure 4. SZ a) E1 b) E2

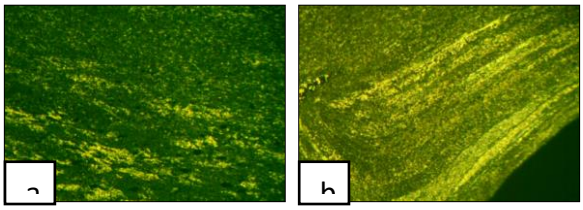

Figure 5. TMAZ-AS a) E1 b) E2

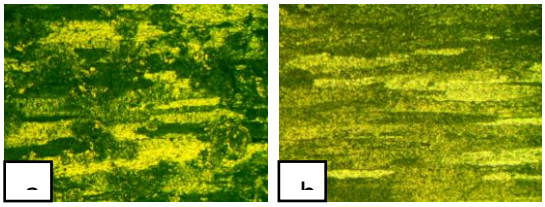

Figure 6. HAZ-AS a) E1 b) E2

3.3 Analysis of Defects

Both the welded samples E1 and E2 comprise of defects. The defects present in E1 are visible at the macro level (see Figure 3a) while that of E2 are visible at the micro level. E1 consists of both tunneling defect(refer Figure 7) as well as hooking defect, whereas E2 contains only hooking as shown in Figure 8. The tunneling defect arises due to a number of significant factors such as inappropriate process parameters, inadequate mixing, applied pressure, insufficient material flow or movement due to tool design etc. [22, 23, 24, 25]. The tunneling defect leads to a decrease in local cross-section area of the welded joint and in turn decreasing the load carrying capacity of the welds. In the present study, the primary reason for the formation of tunneling defect is due to insufficient heat experienced by the base materials at a lower rotational speed in E1. As the rotational speed was increased in E2, the tunnel defect was eliminated which suggests that higher heat input leads to better softening of base materials and in turn a decreased flow stress, which eventually promotes better mixing of the base materials, completing the joint.

Hooking defect was observed in both the samples E1 and E2. It is among the most favorable defects formed during FSW of lap joints. Generally, it appears at the TMAZ on the AS but sometimes it can be observed on both the AS and RS [26]. During FSW, the material undergoes upward extrusion action at the AS and downward forging action at the RS. This repetitive action of upward and downward movement of the base materials during welding results in formation of a hook type feature, known as the hooking defect [26]. Hooking defect is influenced by a number of parameters. In the present work, hooking defect is due to insufficient pin diameter which deters the flow of base material. This defect is not observed in the HAZ because HAZ does not undergo plastic deformation and is only affected by the thermal cycle.

3.4 Tensile Strength

The tensile strengths for samples E1 and E2 are 42.2 MPa and 78.5 MPa respectively. The lower strength in E1 is attributed to the presence of both tunnel defect and hooking defect. The defect site acts as point possessing lowest cross-section and eventually becoming the sites for stress-concentration. The crack initiated from the tunneling defect and ultimately reached the hooking defect thereby giving very low joint efficiency. On the other hand in E2, due to higher rotational speed leading to a higher thermal cycle, enhanced material movement leads to no tunneling defect. Hence, for E2 a better joint efficiency of approximately 57% is achieved. This decrease in joint efficiency is accredited to the presence of defects in both welded samples.

3.5 Microhardness

The microhardness plots for the horizontal and vertical plates are shown in Figure 9a and 9b respectively. The graphs depict the effect of rotational speed on the microhardness for the given samples. The hardness in SZ as well for TMAZ and HAZ on RS is higher for E1 which justifies the hall-petch relationship. The maximum value of hardness was observed to be Also higher rotational speed in E2 contributes to dissolution and coarsening of strengthening precipitates which in turn is responsible for the respective hardness trend. Whereas on the AS higher value of hardness is for E2.

For the vertical plates, the heating effect dominates which leads to grain coarsening. The coarsened grains are present in the vicinity of the SZ up to a distance of 1-1.5 mm, which explains the decrease in hardness for E2.

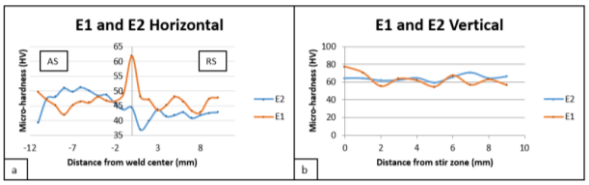

Figure 9: Microhardness a) Horizontal Plate b) Vertical Plate

4. Conclusion

Based on the above study, the following conclusions are drawn:

- Material mixing is observed for different rotational speeds.
- Microhardness values decrease for an increase in thermal cycle corresponding to coarser grains.
- Maximum hardness value was observed to be 61.8 HV.

- The defect was eliminated at higher rotational speed.
- 57% joint efficiency is obtained for sample devoid of tunneling defect.

References

1. Thomas, W.M., Nicholas, E.D., Needham, J.C., Murch, M.G., Temple-Smith, P. and Dawes, C.J., 1991. *International patent no*. PCT/GB92/02203.
2. Su, J.Q., Nelson, T.W., Mishra, R. and Mahoney, M., 2003. Microstructural investigation of friction stir welded 7050-T651 aluminium. *Acta materialia*, *51*(3), pp.713-729.Rhodes CG, Mahoney MW, Bingel WH (1997) Effects of frictionstir welding on microstructure of 7075 aluminum. Scripta Mater36:69–75
3. Mahoney, M.W., Rhodes, C.G., Flintoff, J.G., Bingel, W.H. and Spurling, R.A., 1998. Properties of friction-stir-welded 7075 T651 aluminum. *Metallurgical and materials transactions A*, *29*(7), pp.1955-1964.
4. Leinart, T.J. and Grylls, R.J., 1999. Proc. 1st Int. Symp. FSW, Thousand Oaks, CA.
5. Strombrek, A.V., dos Santos, J.F., Torster, F., Laureano, P. and Kocak, M., 1999. Proc. 1st Int. Symp. FSW, Thousand Oaks, CA.
6. Donne, C.D., Braun, R., Staniek, G., Jung, A. and Kaysser, W.A., 1998. Microstructural, mechanical and corrosive properties of friction stir welded aluminium joints. *Materialwissenschaft Und Werkstofftechnik*, *29*(10), pp.608-616.
7. Midling, O.T., 1994. Proc. 4th Int. Conf. Aluminium Alloys, Atlanta, GA.
8. Sato, Y.S., Urata, M., Kokawa, H. and Ikeda, K., 2003. Hall–Petch relationship in friction stir welds of equal channel angular-pressed aluminium alloys. *Materials Science and Engineering: A*, *354*(1-2), pp.298-305.
9. Berbon, P.B., Bingel, W.H., Mishra, R.S., Bampton, C.C. and Mahoney, M.W., 2001. Friction stir processing: a tool to homogenize nanocomposite aluminum alloys.
10. Lee, W.B., Yeon, Y.M. and Jung, S.B., 2003. The improvement of mechanical properties of friction-stir-welded A356 Al alloy. *Materials Science & Engineering A*, *355*(1-2), pp.154-159.
11. Ferraris, S. and Volpone, L.M., 2005, October. Aluminium alloys in third millennium shipbuilding: materials, technologies, perspectives. In *The Fifth International Forum on Aluminium Ships, Tokyo, Japan*.
12. Teng, T.L., Fung, C.P., Chang, P.H. and Yang, W.C., 2001. Analysis of residual stresses and distortions in T-joint fillet welds. *International Journal of Pressure Vessels and Piping*, *78*(8), pp.523-538.
13. Mashiri, F.R., Zhao, X.L. and Grundy, P., 2004. Stress concentration factors and fatigue behaviour of welded thin-walled CHS–SHS T-joints under in-plane bending. *Engineering Structures*, *26*(13), pp.1861-1875.
14. Fratini, L., Buffa, G. and Shivpuri, R., 2009. Influence of material characteristics on plastomechanics of the FSW process for T-joints. *Materials & Design*, *30*(7), pp.2435-2445.
15. Zhao, Y., Zhou, L., Wang, Q., Yan, K. and Zou, J., 2014. Defects and tensile properties of 6013 aluminum alloy T-joints by friction stir welding. *Materials & Design*, *57*, pp.146-155.
16. Cui, L., Yang, X., Zhou, G., Xu, X. and Shen, Z., 2012. Characteristics of defects and tensile behaviors on friction stir welded AA6061-T4 T-joints. *Materials Science and Engineering: A*, *543*, pp.58-68.
17. Heidarzadeh, A., Jabbari, M. and Esmaily, M., 2015. Prediction of grain size and mechanical properties in friction stir welded pure copper joints using a thermal model. *The International Journal of Advanced Manufacturing Technology*, *77*(9-12), pp.1819-1829.
18. Ahmed, M.M.Z., Ataya, S., Seleman, M.E.S., Ammar, H.R. and Ahmed, E., 2017. Friction stir welding of similar and dissimilar AA7075 and AA5083. *Journal of Materials Processing Technology*, *242*, pp.77-91.
19. Zhang, Z., Wu, Q., Grujicic, M. and Wan, Z.Y., 2016. Monte Carlo simulation of grain growth and welding zones in friction stir welding of AA6082-T6. *Journal of materials science*, *51*(4), pp.1882-1895.
20. Khan, N.Z., Ubaid, M., Siddiquee, A.N., Khan, Z.A., Al-Ahmari, A., Chen, X. and Abidi, M.H., 2018. Microstructural features of friction stir welded dissimilar Aluminium alloys AA2219-AA7475. *Materials Research Express*, *5*(5), p.056531.
21. Zhao, Y., Zhou, L., Wang, Q., Yan, K. and Zou, J., 2014. Defects and tensile properties of

6013 aluminum alloy T-joints by friction stir welding. *Materials & Design*, *57*, pp.146-155.

22. Kim, Y.G., Fujii, H., Tsumura, T., Komazaki, T. and Nakata, K., 2006. Three defect types in friction stir welding of aluminum die casting alloy. *Materials Science and Engineering: A*, *415*(1-2), pp.250-254..
23. Kumar, K.S.V.K. and Kailas, S.V., 2008. The role of friction stir welding tool on material flow and weld formation. *Materials Science and Engineering: A*, *485*(1-2), pp.367-374.
24. Zettler, R., Vugrin, T. and Schmücker, M., 2010. Effects and defects of friction stir welds. In *Friction Stir Welding* (pp. 245-276). Woodhead Publishing.
25. Khan, N.Z., Siddiquee, A.N. and Khan, Z.A., 2017. *Friction Stir Welding: Dissimilar Aluminium Alloys*. CRC Press.